Degree and state of polarization of the time-integrated coherent four-wave mixing signal from semiconductor multiple quantum wells

Shekhar Patkar, A. E. Paul, W. Sha, J. A. Bolger, and Arthur L. Smirl
Laboratory for Photonics and Quantum Electronics, 100 Iowa Advanced Technology Laboratories, University of Iowa, Iowa City, Iowa 52242-1000
(Received 20 December 1994)

All four of the Stokes parameters of the time-integrated degenerate four-wave mixing signal from a $GaAs/Al_xGa_{1-x}As$ multiple quantum well are measured as a function of the relative angle between the linear polarizations of the pump and the probe and of the incident fluence, thus completely characterizing the polarization state of the signal. The degree to which the signal is polarized, the ellipticity, and the orientation of the polarization ellipse are found to be strongly dependent on the orientation of the incident polarizations and on fluence. The principal features can be qualitatively understood in terms of a simple model that includes density-dependent dephasing and local-field corrections.

I. INTRODUCTION

Degenerate four-wave mixing (FWM) has been shown to be a powerful tool for studying fundamental coherent transient processes in semiconductors.[1] Recent studies[2–7] indicate that the polarization selection rules for FWM can be very useful in discriminating between various proposed models for these processes, particularly in delineating the roles of excitation-induced dephasing (EID),[2,4,7] of the interaction-induced field (or the so-called local-field correction, LFC)[8–14] and of biexcitons.[15–20] These polarization studies have tended to focus on the dependence of the magnitude of the FWM signal on the polarization states of the input pulses, and the polarization state of the FWM signal itself has been largely ignored. Recent observations,[2,3,5] however, have stimulated interest in the polarization state of the FWM signal. Such time-integrated (TI) FWM experiments[3] performed on $GaAs/Al_xGa_{1-x}As$ multiple quantum wells (MQW's) have demonstrated that the polarization of the FWM signal has a previously unexpected dependence on the relative polarizations of the input pulses, which has subsequently been explained in terms of EID.[2] In experiments performed to date, however, the degree and state of polarization of the FWM signal have been only partially determined, as we shall discuss.

In this paper, we describe the measurement of all four Stokes parameters that completely characterize the degree and state of polarization of the TI-FWM signal in a $GaAs/Al_xGa_{1-x}As$ MQW as a function of the angle between the linear polarizations of the two input beams and as a function of excitation fluence. We demonstrate that the ellipticity, the orientation of the polarization ellipse, and the degree of polarization each vary dramatically with the incident polarizations and with the fluence, and we show that all of the observed tendencies agree qualitatively with a model that includes exciton-exciton interactions in a phenomenological way. In contrast to previous results that were interpreted in terms of EID alone, our results indicate that both EID and LFC must be included.

II. MEASUREMENT OF STOKES PARAMETERS

The geometry used for our measurements is illustrated in Fig. 1. Specifically, a 100-fs pulse (full width at half maximum of the intensity, FWHM) with a spectral width of 15 meV (FWHM) produced by a mode-locked Ti:sapphire laser was divided into two parts. The two parts, one with wave vector $\mathbf{k}_1$ and the other with wave vector $\mathbf{k}_2$, were spatially overlapped in the MQW with a small external angle ($\sim 10°$) between the two beams, as shown in Fig. 1(a). For the measurements described here, the time delay τ_{12} between the two pulses was set to zero and calibrated by using the autocorrelation signal from frequency up-conversion in a second-harmonic generation (SHG) crystal. The $\mathbf{k}_2$ pulse was arranged to be linearly and s polarized, with polarization vector $\mathbf{E}_2$

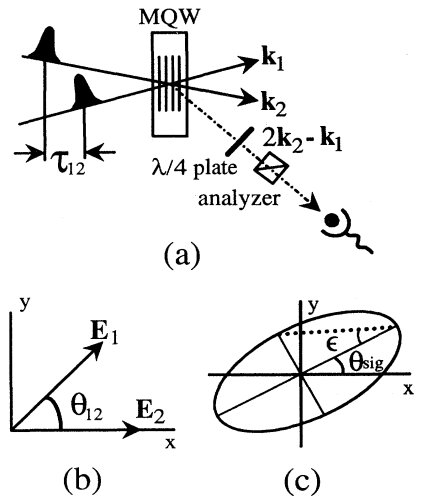

FIG. 1. (a) Experimental geometry for measuring the Stokes parameters of the time-integrated degenerate four-wave mixing signal, (b) relative orientation of the input linear polarizations, and (c) schematic of the polarization ellipse showing the azimuth angle θ_{sig} and the ellipticity angle ϵ.

defining the x axis, and the linear polarization $\mathbf{E}_1$ of the $\mathbf{k}_1$ pulse was rotated by an angle θ_{12} with respect to $\mathbf{E}_2$, as shown in Fig. 1(b).

With the quarter-wave plate removed from the FWM path, four linear components of the TI-FWM signal (I_x, I_y, I_{+45}, and I_{-45}, corresponding to light polarized along the x axis, y axis, and at $+45°$ and $-45°$ to the x axis, respectively) were measured. Then with the quarter-wave plate in place, two circular components (I_+ and I_-, corresponding to left and right circularly polarized light, respectively) were measured. The actual procedure for obtaining these six components was to measure the TI-FWM signal as the analyzer was rotated through 180° with, and without, the quarter-wave plate in place and, then, to extract these six components from the resulting fluence versus analyzer angle curves. This procedure provides maximum sensitivity and a degree of redundancy. The four Stokes parameters that completely determine the polarization were then computed from these six components using the following well-known definitions:[21] $S_0=I_x+I_y=I_{+45}+I_{-45}=I_++I_-$, $S_1=I_x-I_y=2I_x-S_0$, $S_2=I_{+45}-I_{-45}=2I_{+45}-S_0$, and $S_3=I_+-I_-=2I_+-S_0$. Clearly, all Stokes parameters can be obtained from the four components I_x, I_y, I_{+45}, and I_+; however, measurement of the additional two enabled us to confirm internal self-consistency by comparing all possible combinations resulting in the four Stokes parameters.

The degree of polarization P, the azimuthal angle $\theta_{\rm sig}$, and the ellipticity angle ε that determine the polarization ellipse [as shown in Fig. 1(c)] were then calculated from the Stokes parameters using the expressions[21] $P=(S_1^2+S_2^2+S_3^2)^{1/2}/S_0$, $\sin(2\varepsilon)=S_3/(S_1^2+S_2^2+S_3^2)^{1/2}$, and $\tan(2\theta_{\rm sig})=S_2/S_1$. From these definitions, and from Fig. 1(c), it can be seen that P corresponds to the fraction of light that is polarized, that $\theta_{\rm sig}$ determines the orientation of the major axis of the polarization ellipse with respect to the x axis, and that ε is a measure of the ratio of the minor axis to the major axis of the polarization ellipse (e.g., $\varepsilon=\pm45°$ indicates that the polarized component of the light is circularly polarized, while $\varepsilon=0°$ indicates that it is linearly polarized). In previous investigations of the polarization dependence of the FWM signal, subsets of the Stokes parameters have been reported. For example, the azimuth angle,[2,3,5] the degree of linear polarization (S_1/S_0), and the degree of circular polarization[2] (S_3/S_0) have each been separately measured, but we are unaware of any report of the complete determination of all four Stokes parameters.

The MQW sample studied here consists of 50 periods of 10-nm-wide GaAs wells separated by 7.5-nm-wide $Al_{0.3}Ga_{0.7}As$ barriers. The measurements were performed at 80 K. At this temperature, the heavy-hole exciton has an absorption linewidth of 1.4 meV, and the separation between heavy-hole (hh) and light-hole (lh) excitons is 11.2 meV. The laser was tuned 1 meV below the hh exciton, where the ratio of the number of hh excitons excited to the number of lh excitons was roughly 10:1. Moreover, at 80 K, the hh exciton was at least partially homogeneously broadened by phonon scattering, and, at all but the lowest fluences used here, it was completely homogeneously broadened by the density-dependent dephasing. This assertion of homogeneous broadening is based on a detailed study of the excitonic and FWM linewidths as a function of temperature and excitation level, and was further verified by the absence of echolike behavior in the time-resolved FWM signal as a function of the time delay τ_{12}.

Using the procedure described above, measurements of the degree of polarization P, the azimuthal angle $\theta_{\rm sig}$, and the ellipticity ε of the TI-FWM signal were performed as a function of angle θ_{12} between the two incident polarizations and as a function of incident fluence. Representative results are shown in Fig. 2 for three selected fluences. The high (2.8 μJ cm^{-2}) and low (0.2 μJ cm^{-2}) fluences correspond, respectively, to hh exciton densities of 2×10^{10} and 1.5×10^{9} cm^{-2}. The contrasting behavior of the azimuthal angle $\theta_{\rm sig}$ as a function of θ_{12} for high and low fluences has been reported previously,[2,3,5] and the results shown in Fig. 2(a) confirm these previous observations. Specifically, at the highest fluences, the azimuth angle follows the rule $\theta_{\rm sig}=-\theta_{12}$ (which is the expected behavior for two independent, uncoupled excitonic spin states[2,3,5]). At the lowest fluences, however, the azimuth angle makes a sudden transition through almost 90° at a critical angle of $\theta_{12}\approx60°$ [which has been interpreted in

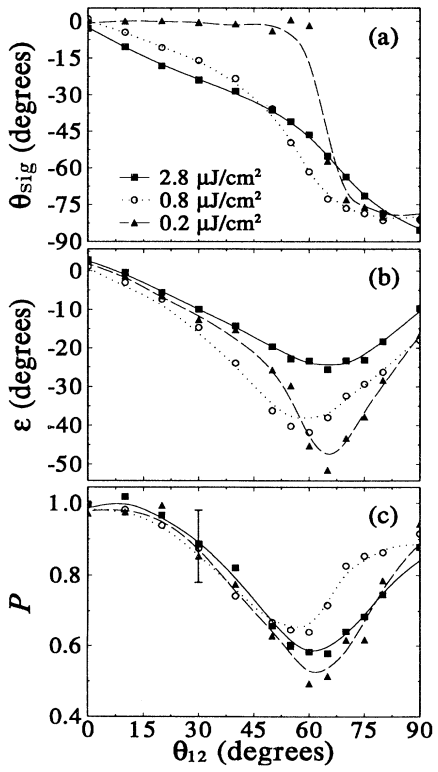

FIG. 2. Measurements of (a) the azimuth angle $\theta_{\rm sig}$, (b) the ellipticity angle ε, and (c) the degree of polarization P as a function of the angle θ_{12} between the two input polarizations for fluences of 0.2 (triangles), 0.8 (circles), and 2.8 μJ cm^{-2} (squares).

terms of EID (Ref. 2)]. The intermediate fluence illustrates that the change from low-density to high-density behavior is a gradual one.

By comparison, the ellipticity angle ε [see Fig. 2(b)] initially begins at 0° (linear polarization) and increases in magnitude with increasing θ_{12}, until it reaches a maximum ellipticity at approximately the same position as the sudden transition in the azimuthal angle $\theta_{\rm sig}$ (i.e., $\theta_{12}\approx 60°$). The ellipticity angle ε also increases with decreasing fluence, with a maximum ellipticity of $-45°$ (circular polarization) observed for some angles at the lowest fluence. The degree of polarization P also initially decreases with increasing θ_{12}, and a depolarization of almost 30% is observed at about the same point as the one at which the ellipticity is a maximum. At this time, we do not assign any significance to the variations of P with fluence, since this parameter depends on the independent measurement of all four Stokes parameters and is therefore subject to the largest uncertainty [as indicated by the error bar in Fig. 2(c)].

The trends discussed in the previous two paragraphs are more evident if we simultaneously consider the behavior of the azimuthal $\theta_{\rm sig}$ and ellipticity ε angles [i.e., the data in Figs. 2(a) and 2(b)] by sketching the corresponding polarization ellipses, as we have done in Fig. 3. Again, notice that, for each fixed fluence, the ellipticity increases then decreases with increasing θ_{12}, and that the azimuthal angle rotates from $+x$ to $-y$. Also, for each fixed angle between the input polarizations, the ellipticity increases with decreasing fluence. From these ellipses, it is readily apparent that changes that appeared sudden and dramatic in Fig. 2 (for example, the jump in the azimuthal angle $\theta_{\rm sig}$ near $\theta_{12}\approx 60°$ at the lowest fluence) are really part of a smooth and continuous trend with fluence and polarization angle θ_{12}. It should be emphasized that the ellipses drawn in Fig. 3 only represent the polarized portion of the FWM signal, and that there is also a significant unpolarized component that is largest when the ellipticity is largest.

Finally, in addition to measuring the Stokes parameters, we repeated the tests for biexcitons described in Ref. 16, and the selection rules for parallel, perpendicular, and copolarized pulses were not consistent with those of the biexciton. Despite the recent reports of the importance of biexcitonic effects,[15–20] this is not an unexpected result for our experimental conditions. For the measurements shown in Fig. 2, the hh line width was measured to range from ~ 1.6 to 4.0 meV, while the biexciton binding energy is expected to be of the order of 1 meV.

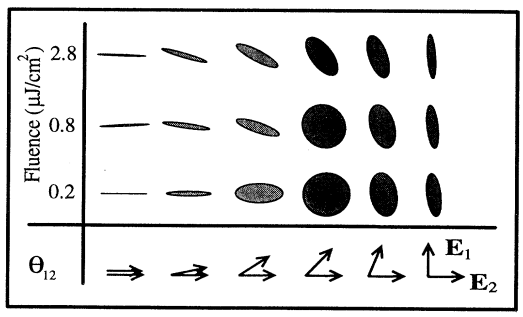

FIG. 3. Polarization ellipses for selected angles θ_{12} extracted from Fig. 2.

III. COMPARISON WITH THEORY

Excluding the biexcitonic effects, the simplest description of the excitation of heavy holes in a homogeneously broadened semiconductor is to use the optical Bloch equations for two uncoupled two-level systems to describe the σ_+ and σ_- excitonic transitions (e.g., Ref. 22) and to include many-body effects phenomenologically (although a complete theoretical description of many-body effects should certainly be based on the solution of the full semiconductor Bloch equations).[2,7,13,14,23] The two main many-body effects that we wish to include are the excitation-induced dephasing (EID) and the renormalization of the Rabi energy or so-called local-field correction (LFC). The density-dependent dephasing can be introduced by expanding the dephasing rate for the hh excitons $\gamma(n)$ in a Taylor series and keeping the first two terms:[2,4]

$$\gamma(n)=\gamma(n_0)+\frac{\partial\gamma}{\partial n}(n-n_0)\ , \tag{1}$$

where $n(n_0)$ is the total (initial) carrier density. The renormalization of the Rabi energy (LFC) is included by adding to the field a term proportional to the total material polarization:[8,24]

$$\mathbf{E}_{\rm LOC}=\mathbf{E}+L\mathbf{P}\ , \tag{2}$$

where $\mathbf{P}$ is the total material polarization and L is a local-field parameter. After making these substitutions into the optical Bloch equations, one finds the parameters of interest to be[25] the EID parameter $\eta=\hbar N(\partial\gamma/\partial n)$ and the LFC parameter $\xi=|\mu_{\rm hh}|^2NL$, where N is the total number of oscillators that can be excited in each spin state and $\mu_{\rm hh}$ is the hh dipole matrix element. Both the EID parameter and LFC parameter as defined here have the dimensions of energy.

In order to obtain the simplest description of our FWM experiments and to obtain a closed-form solution, we assume that the pulses in the directions $\mathbf{k}_1$ and $\mathbf{k}_2$ have delta-function time dependences given by $\delta(t-\tau_{12})$ and $\delta(t)$, respectively. The two fields are assumed to have linear polarizations oriented at an angle θ_{12} with respect to each other [as in Fig. 1(b)]. Under these circumstances, one can readily solve the optical Bloch equations for the third-order polarization in the $2\mathbf{k}_2-\mathbf{k}_1$ direction at time t:

$$\mathbf{P}^{(3)}_{2\mathbf{k}_2-\mathbf{k}_1}(t)=\frac{-2iN\mu_{\rm hh}^4E_2^2E_1^*}{\hbar^3}\left\{\Theta(t)\Theta(\tau_{12})e^{-(i\Omega+\gamma)t}e^{(i\Omega-\gamma)\tau_{12}}\left[\begin{pmatrix}\cos\theta_{12}\\-\sin\theta_{12}\\0\end{pmatrix}(1+i\xi t/\hbar)+\begin{pmatrix}\cos\theta_{12}\\0\\0\end{pmatrix}\eta t/\hbar\right]\right.$$
$$\left.+\Theta(t+\tau_{12})\Theta(-\tau_{12})e^{-(i\Omega+\gamma)t}e^{(i\Omega+\gamma)\tau_{12}}\left[\begin{pmatrix}\cos\theta_{12}\\-\sin\theta_{12}\\0\end{pmatrix}i\xi(t+\tau_{12})/\hbar+\begin{pmatrix}\cos\theta_{12}\\0\\0\end{pmatrix}\eta(t+\tau_{12})/\hbar\right]\right\}. \quad (3)$$

Here $\Omega=\Omega_{\rm hh}-\omega_L-\xi/\hbar$, where $\Omega_{\rm hh}$ is the circular frequency corresponding to the transition energy of the hh exciton, and ω_L is the frequency of the laser and Θ is the Heaviside function. This expression can then be used to calculate the Stokes parameters of the FWM signal as a function of the relative angle θ_{12} between the polarizations of the two input pulses in the low fluence limit.

In Fig. 4, we show the results of calculating the azimuthal angle $\theta_{\rm sig}$, the ellipticity angle ε, and the degree of depolarization $(1-P)$ in the absence of local-field corrections ($\xi=0$ meV). Without EID [$\eta=0$ meV in Fig. 4(a)], the azimuth angle behaves as expected for two uncoupled two-level (2×2) systems (i.e., $\theta_{\rm sig}=-\theta_{12}$). However, as the strength of EID is increased, $\theta_{\rm sig}$ tends to remain small for small θ_{12} until, for θ_{12} between 60° and 70°, it abruptly changes to 90°—in agreement with our observations. This abrupt change is simply a consequence of the fact that EID does not contribute for orthogonally polarized pulses, and thus it enhances the x component of the FWM signal but not the y component, as is evident from Eq. (3).

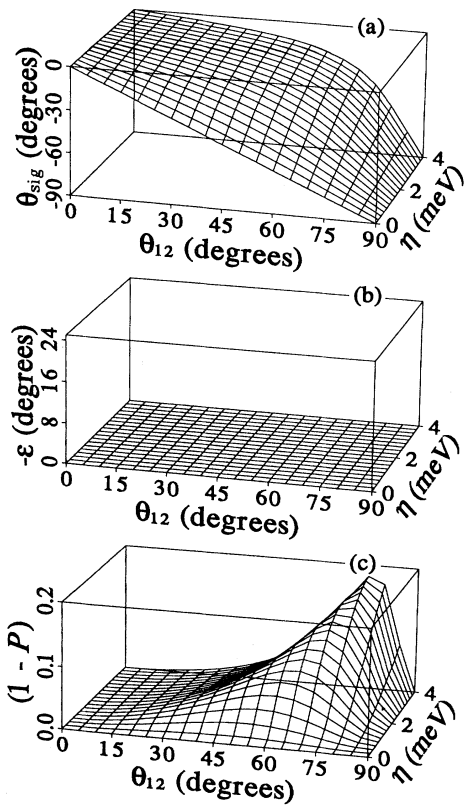

FIG. 4. Calculated values for (a) the azimuth angle $\theta_{\rm sig}$, (b) the ellipticity angle ε, and (c) the degree of depolarization $(1-P)$ as a function of the angle θ_{12} between the two input polarizations and as a function of the EID parameter η with the local-field parameter $\xi=0$ meV.

However, in the absence of any local-field correction, the ellipticity [shown in Fig. 4(b)] is zero for all values of the EID parameter. This result is to be expected since elliptically polarized light can only be generated if a phase shift is introduced between the x and y components of the FWM field. Because the EID and LFC originate from the imaginary and real parts of the exciton self-energy,[7] they enter the solution with different phases. As can be seen in Eq. (3), EID enters the solution with the same phase as the prompt decay terms, while the LFC enters with a phase factor of $\exp(i\pi/2)$. Therefore, in the absence of the LFC, there can be no phase difference between the x and y components of the signal, and hence, no ellipticity. Nevertheless, EID can lead to a depolarization approaching 20%, as shown in Fig. 4(c). Consequently, we see that EID can account qualitatively for the observed variations in the azimuthal angle $\theta_{\rm sig}$ and for the degree of depolarization $(1-P)$, but, when acting alone, it cannot account for the observed ellipticity ε.

A similar set of results are shown in Fig. 5 where we now include LFC. The results for the LFC acting alone are represented by the curves produced by choosing $\eta=0$ meV. In the absence of EID (because the LFC does not couple the two two-level systems and because it contributes equally to both x and y components of the FWM signal), the polarization of the FWM signal remains linear ($\varepsilon=0°$) with the azimuthal angle determined by $\theta_{\rm sig}=-\theta_{12}$, and the FWM signal experiences no depolarization regardless of the strength chosen for the LFC. Consequently, the LFC acting alone will reproduce none of the measured tendencies in the Stokes parameters.

When both the EID and LFC are included, all characteristics of the FWM polarization are reproduced as shown in Fig. 5 for $\eta\neq0$. The knee in the $\theta_{\rm sig}$ versus θ_{12} curve and the depolarization are still primarily the result of the EID. However, since the LFC contributes equally to both the x and y components of the signal, it has the net effect of reducing the enhancement of the x component due to EID. As a result, the deviation of the azimuth angle from the relation $\theta_{\rm sig}=-\theta_{12}$ becomes less severe when the LFC is included. Nevertheless, it is necessary to include both the LFC and EID in order to

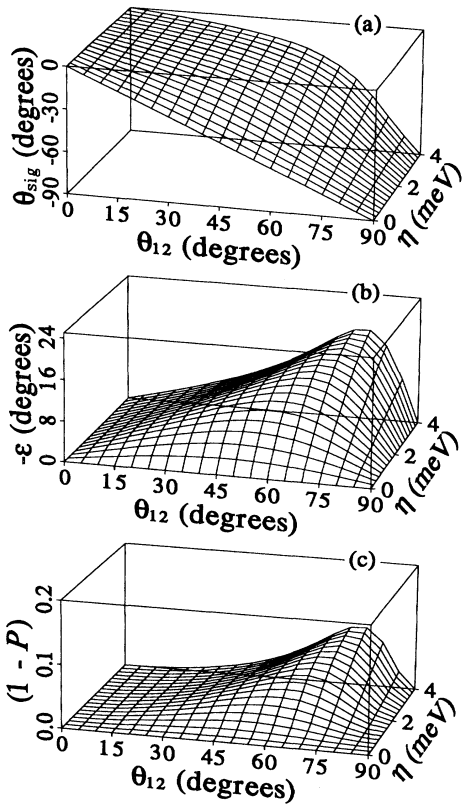

FIG. 5. Calculated values for (a) the azimuth angle θ_{sig}, (b) the ellipticity angle ε, and (c) the degree of depolarization $(1-P)$ as a function of the angle θ_{12} between the two input polarizations and as a function of the EID parameter η with the local-field parameter $\xi=1$ meV.

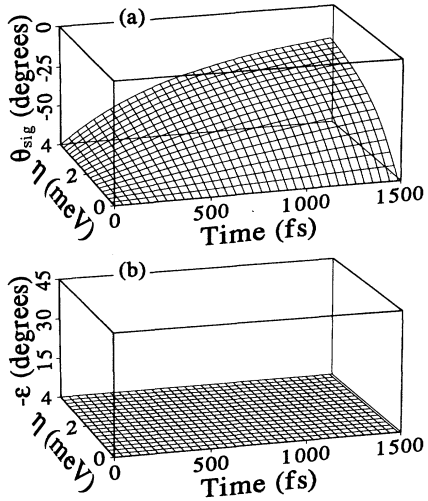

FIG. 6. Calculated values for (a) the azimuth angle θ_{sig} and (b) the ellipticity angle ε as a function of time following excitation and as a function of the EID parameter η, for a fixed angle between the input polarizations ($\theta_{12}=75°$) and with the local-field parameter $\xi=0$ meV.

obtain the desired ellipticity as the two enter Eq. (3) in quadrature. In the absence of either the EID or LFC, the light would be linearly polarized. Note that the LFC and the prompt decay also enter Eq. (3) out of phase by $\pi/2$; however, together they introduce the same phase factor in the x and y components of the signal, and, therefore, produce no ellipticity without EID.

We wish to emphasize that the depolarization shown in Figs. 4 and 5 does not imply that the FWM signal has a random component to its polarization. Rather, we believe that the light is deterministically polarized at each instant of time, as dictated by Eq. (3); however, since the relative EID and LFC contributions change in time, so will the state of polarization. Consequently, the averaging of the polarization introduced by time integrating the signal yields a degree of polarization less than 1. This process is illustrated in Figs. 6 and 7, where we show the azimuth and ellipticity angles as a function of real time for a fixed angle ($\theta_{12}=75°$) between the input polarizations both without the LFC ($\xi=0$ meV) and with the LFC ($\xi=1$ meV). As previously discussed, without EID, the light remains linearly polarized, does not rotate in time, and therefore produces no depolarized component to the signal. With EID, but without the LFC (Fig. 6), the signal remains linearly polarized ($\varepsilon=0°$), but rotates in time as the contribution from the EID evolves. By comparison, when both the EID and LFC are included in the model (Fig. 7), the signal rotates (i.e., the azimuthal angle changes) and the phase difference between its x and y components changes with time. This time dependence in the azimuth and ellipticity angles leads to a component of unpolarized light in the TI-FWM signal.

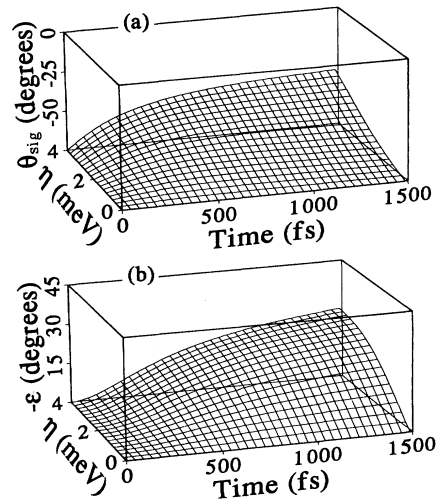

FIG. 7. Calculated values for (a) the azimuth angle θ_{sig} and (b) the ellipticity angle ε as a function of time following excitation and as a function of the EID parameter η, for a fixed angle between the input polarizations ($\theta_{12}=75°$) and with the local-field parameter $\xi=1$ meV.

IV. SUMMARY AND CONCLUSIONS

In summary, we have measured all four Stokes parameters of the time-integrated FWM signal from a multiple quantum well (MQW) as a function of the angle between the two linearly polarized incident pulses and as a function of fluence. In this way, we have completely specified the polarization state of the scattered light. As a result, we have not only verified that the direction of polarization (i.e., the azimuthal angle of the polarization ellipse) has a complicated (but reproducible) dependence on the incident polarization and fluence (as previously reported),[2,3,5] but we have shown that the ellipticity and the time-integrated degree of polarizability are also complicated functions of the same parameters. In addition, we have compared our measurements to a simple model based on the optical Bloch equations for two independent two-level systems (the so-called 2×2 model) in which the EID and LFC were included phenomenologically. Such a model qualitatively reproduces all of the observed fundamental dependences of the state of polarization of the FWM signal on the relative polarizations of the incident pulses. Using this model, we have shown that the variation in the behavior of the azimuth angle (with fluence and incident polarization) is dominated by EID and is consistent with a decrease in the influence of the EID as the density is increased. We have also shown that the presence of EID alone is sufficient to produce an unpolarized component in the time-integrated Stokes parameters, but that both the LFC and EID are required to produce the observed elliptically polarized light. Moreover, our parametric studies show that the LFC suppresses the polarization rotation and the depolarization associated with EID, making the density dependence of both the EID and LFC important. Finally, the depolarized component in the TI-FWM signal is explained in terms of the temporal integration of the time-dependent azimuth angle and the ellipticity. This time dependence is shown to originate from the temporal imbalance between the x and y components of the signal introduced by the EID and LFC.

ACKNOWLEDGMENTS

This work was supported in part by the National Science Foundation, the Office of Naval Research and the National Institute for Standards and Technology.

[1] *Coherent Optical Interactions in Semiconductors,* edited by R. T. Phillips (Plenum, New York, 1994), and references therein.
[2] Y. Z. Hu, R. Binder, S. W. Koch, S. T. Cundiff, H. Wang, and D. G. Steel, Phys. Rev. B **49**, 14 382 (1994).
[3] R. Eccleston, J. Kuhl, D. Bennhardt, and P. Thomas, Solid State Commun. **86**, 93 (1993).
[4] H. Wang, K. Ferrio, D. G. Steel, Y. Z. Hu, R. Binder, and S. W. Koch, Phys. Rev. Lett. **71**, 1261 (1993).
[5] K. Bott, O. Heller, D. Bennhardt, S. T. Cundiff, P. Thomas, E. J. Mayer, G. O. Smith, R. Eccleston, J. Kuhl, and K. Ploog, Phys. Rev. B **48**, 17 418 (1993).
[6] S. T. Cundiff, H. Wang, and D. G. Steel, Phys. Rev. B **46**, 7248 (1992).
[7] T. Rappen, U.-G. Peter, M. Wegener, and W. Schäfer, Phys. Rev. B **49**, 10 774 (1994).
[8] M. Wegener, D. S. Chemla, S. Schmitt-Rink, and W. Schäfer, Phys. Rev. A **42**, 5675 (1990).
[9] K. Leo, E. O. Göbel, T. C. Damen, J. Shah, S. Schmitt-Rink, W. Schäfer, J. E. Müller, K. Köhler, and P. Ganser, Phys. Rev. B **44**, 5726 (1991).
[10] K. Leo, M. Wegener, J. Shah, D. S. Chemla, E. O. Göbel, T. C. Damen, S. Schmitt-Rink, and W. Schäfer, Phys. Rev. Lett. **65**, 1340 (1990).
[11] D. S. Kim, J. Shah, T. C. Damen, W. Schäfer, F. Jahnke, S. Schmitt-Rink, and K. Köhler, Phys. Rev. Lett. **69**, 2725 (1992).
[12] S. Weiss, M.-A. Mycek, J.-Y. Bigot, S. Schmitt-Rink, and D. S. Chemla, Phys. Rev. Lett. **69**, 2685 (1992).
[13] C. Stafford, S. Schmitt-Rink, and W. Schäfer, Phys. Rev. B **41**, 10 000 (1990).
[14] W. Schäfer, F. Jahnke, and S. Schmitt-Rink, Phys. Rev. B **47**, 11 359 (1990).
[15] D. S. Kim, J. Shah, T. C. Damen, L. N. Pfeiffer, and W. Schäfer, Phys. Rev. B **50**, 5775 (1994).
[16] H. Wang, J. Shah, T. C. Damen, and L. N. Pfeiffer, Solid State Commun. **91**, 869 (1994).
[17] R. Raj, I. Abram, and J. A. Levenson, Solid State Commun. **81**, 51 (1992).
[18] S. Bar-Ad and I. Bar-Joseph, Phys. Rev. Lett. **68**, 349 (1992).
[19] D. Lovering, R. T. Phillips, and G. J. Denton, Phys. Rev. B **68**, 1880 (1992).
[20] B. F. Feuerbacher, J. Kuhl, and K. Ploog, Phys. Rev. B **42**, 2429 (1991).
[21] G. G. Stokes, Trans. Cambridge Philos. Soc. **9**, 399 (1852). For a detailed description, see R. M. A. Azzam and N. M. Bashara, *Ellipsometry and Polarized Light* (North-Holland, Amsterdam, 1988).
[22] S. Schmitt-Rink, D. Bennhardt, V. Heuckeroth, P. Thomas, P. Haring, G. Maidorn, H. Bakker, K. Leo, D.-S. Kim, J. Shah, and K. Köhler, Phys. Rev. B **46**, 10 460 (1992).
[23] M. Lindberg, R. Binder, and S. W. Koch, Phys. Rev. A **45**, 1865 (1992).
[24] S. Schmitt-Rink, S. Mukamel, K. Leo, and D. S. Chemla, Phys. Rev. A **44**, 2124 (1991).
[25] A. E. Paul, W. Sha, S. Patkar, and A. L. Smirl, Phys. Rev. B **50**, 4242 (1995).